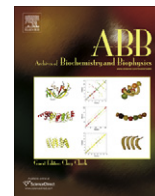




Contents lists available at ScienceDirect

## Archives of Biochemistry and Biophysics

journal homepage: [www.elsevier.com/locate/yabbi](http://www.elsevier.com/locate/yabbi)

## Structure of the two-subsite $\beta$ -D-xylosidase from *Selenomonas ruminantium* in complex with 1,3-bis[tris(hydroxymethyl)methylamino]propane<sup>☆</sup>

Joseph S. Brunzelle<sup>a</sup>, Douglas B. Jordan<sup>b,\*</sup>, Darrell R. McCaslin<sup>c</sup>, Andrzej Olczak<sup>d</sup>, Zdzislaw Wawrzak<sup>e</sup><sup>a</sup>Northwestern University Center for Synchrotron Research, Life Sciences Collaborative Access Team, Department of Molecular Pharmacology and Biological Chemistry, 9700 South Cass Avenue, Argonne, IL 60439, USA<sup>b</sup>Fermentation Biotechnology Research Unit, National Center for Agricultural Utilization Research, U.S. Department of Agriculture, Agricultural Research Service, 1815 North University Street, Peoria, IL 61604, USA<sup>c</sup>Department of Biochemistry, Biophysics Instrumentation Facility, 433 Babcock Drive, University of Wisconsin-Madison, Madison, WI 53706-1544, USA<sup>d</sup>Institute of General and Ecological Chemistry, Technical University of Lodz, ul. Zeromskiego 116, 90-924 Lodz, Poland<sup>e</sup>Department of Biochemistry, Molecular Biology and Cell Biology, Northwestern University, 2205 Tech Drive, Evanston, IL 60208-3500, USA

## ARTICLE INFO

## Article history:

Received 29 January 2008

and in revised form 5 March 2008

Available online 14 March 2008

## Keywords:

Glycoside hydrolase

GH43

 $\alpha$ -L-Arabinofuranosidase

Structure-function

Protein crystallography

Sedimentation equilibrium

## ABSTRACT

The three-dimensional structure of the catalytically efficient  $\beta$ -xylosidase from *Selenomonas ruminantium* in complex with competitive inhibitor 1,3-bis[tris(hydroxymethyl)methylamino]propane (BTP) was determined by using X-ray crystallography (1.3 Å resolution). Most H bonds between inhibitor and protein occur within subsite –1, including one between the carboxyl group of E186 and an N group of BTP. The other N of BTP occupies subsite +1 near K99. E186 (pK<sub>a</sub> 7.2) serves as catalytic acid. The pH (6–10) profile for  $1/K_i^{(BTP)}$  is bell-shaped with pK<sub>a</sub>'s 6.8 and 7.8 on the acidic limb assigned to E186 and inhibitor groups and 9.9 on the basic limb assigned to inhibitor. Mutation K99A eliminates pK<sub>a</sub> 7.8, strongly suggesting that the BTP monocation binds to the dianionic enzyme D14<sup>–</sup>E186<sup>–</sup>. A sedimentation equilibrium experiment estimates a  $K_d$  ( $[dimer]^2/[tetramer]$ ) of  $7 \times 10^{-9}$  M. Similar  $k_{cat}$  and  $k_{cat}/K_m$  values were determined when the tetramer/dimer ratio changes from 0.0028 to 26 suggesting that dimers and tetramers are equally active forms.

© 2008 Elsevier Inc. All rights reserved.

$\beta$ -D-Xylosidase/ $\alpha$ -L-arabinofuranosidase from *Selenomonas ruminantium* (SXA)<sup>1</sup>, a family 43 glycoside hydrolase (GH43), is the best catalyst known for promoting the hydrolysis of 1,4- $\beta$ -xylooligosaccharides [1,2]. By having the highest known  $k_{cat}$  and  $k_{cat}/K_m$  values with xylooligosaccharide substrates, bifunctionality of  $\beta$ -xylosidase (EC 3.2.1.37) and  $\alpha$ -arabinofuranosidase (EC 3.2.1.55) activities [1–5], and good thermal and pH stabilities [5], SXA has potential utility in industrial processes for saccharification of herbaceous biomass (arabinoxylan fraction) to simple sugars that can be fermented to ethanol and other products [6,7].

A common structural feature of enzymes belonging to glycoside hydrolase families 32, 43, 62, and 68 is a 5-bladed  $\beta$ -propeller domain that comprises the catalytic acid and the catalytic base [8–10]. Recently-determined X-ray structures of GH43  $\beta$ -xylosidases from *Bacillus subtilis*, *Bacillus halodurans*, *Clostridium acetobutylicum*, and *Geobacillus stearothermophilus*, which have 53–70% protein sequence identity with SXA, show that the enzymes possess an additional C-terminal  $\beta$ -sandwich domain that serves to close off a portion of the active site to form a pocket. The active-site pocket comprises two subsites (binding capacity for two monosaccharide moieties) and a single route of access for small molecules such as substrate. The additional residues of oligosaccharide substrates, comprising more than two monosaccharide residues, must extend the additional residues beyond subsite +1 of the active-site pocket to bulk solvent [1,3,8]. The structure of a catalytically inactive, site-directed mutant of *G. stearothermophilus*  $\beta$ -xylosidase (PDB ID 2EXK; containing E187G mutation of catalytic acid) in complex with  $\beta$ -1,4-xylobiose [8] has been most useful in modeling the SXA active site. Complementary to the structural information, biochemical studies have established that (a) SXA catalyzes hydrolysis of 4NPX and  $\beta$ -1,4-xylobiose with inversion of stereochemistry implicating a single transition state

<sup>☆</sup> Atomic coordinates and structure factors for  $\beta$ -D-xylosidase from *Selenomonas ruminantium* in complex with 1,3-bis[tris(hydroxymethyl)methylamino]propane have been deposited in the Research Collaboratory for Structural Bioinformatics (<http://www.rcsb.org/pdb>) with the accession code 3C2U.

\* Corresponding author. Fax: +1 309 681 6427.

E-mail address: [douglas.jordan@ars.usda.gov](mailto:douglas.jordan@ars.usda.gov) (D.B. Jordan).

<sup>1</sup> Abbreviations used: SXA,  $\beta$ -D-xylosidase/ $\alpha$ -L-arabinofuranosidase from *S. ruminantium*; 4NPX, 4-nitrophenyl- $\beta$ -D-xylopyranoside; 4NPA, 4-nitrophenyl- $\alpha$ -L-arabinofuranoside; GH, glycoside hydrolase; GH43, glycoside hydrolase family 43; BTP, 1,3-bis[tris(hydroxymethyl)methylamino]propane; SAS, solvent accessible surface; rms, root mean squared;  $M_w$ , weight-average molecular weight;  $M_s$ , sequence molecular weight.

with the catalytic base (D14) serving to activate a water molecule for addition to substrate and the catalytic acid (E186) serving to protonate the leaving group, (b) SXA catalyzes the hydrolysis of a single residue from the nonreducing end of substrate without processivity so that all products of the hydrolysis reaction are removed from the active site before initiating another catalytic cycle [1], (c) the single active site of the SXA protomer is responsible for both the  $\beta$ -xylosidase and  $\alpha$ -arabinofuranosidase activities [1,4], and (d) catalysis is governed by  $pK_a$  5.0 and  $pK_a$  7.2, respectively, assigned to the catalytic base, D14, and the catalytic acid, E186, such that SXA in the D14<sup>-</sup>E186<sup>H</sup> form is catalytically active and SXA in the D14<sup>H</sup>E186<sup>H</sup> and D14<sup>-</sup>E186<sup>-</sup> forms are catalytically inactive [1,3].  $pK_a$  values of the three active-site carboxylic acid residues (D14, D127, and E186) are likely raised by their proximity to one another (within 6 Å);  $pK_a$  5.0, reporting the carboxyl group of D14, is likely made more normal by its close proximity (4.2 Å) to the guanidinium group of R290 and  $pK_a$  7.2, reporting the carboxyl group of E186, is likely made more basic by its close proximity (3.8 Å) to the carboxyl group of D127 [1].

In addition to controlling catalysis, the protonation state of D14 and E186 controls the affinity of SXA for inhibitory monosaccharides, whereas D14<sup>H</sup>E186<sup>H</sup> has no binding affinity for monosaccharides, D14<sup>-</sup>E186<sup>H</sup> and D14<sup>-</sup>E186<sup>-</sup> enzyme forms are capable of binding monosaccharides and the preference for one or the other enzyme forms is monosaccharide dependent [3]. Only D14<sup>-</sup>E186<sup>H</sup> SXA is capable of binding two equivalents of monosaccharide per active site. We have proposed that the negatively charged environment that is confined mostly within subsite -1 of D14<sup>-</sup>E186<sup>-</sup> repels binding of monosaccharides therein and leaves subsite +1 open for binding of a single monosaccharide per active site [3].

None of the saccharide inhibitors have been found to bind only to the D14<sup>-</sup>E186<sup>-</sup> form of SXA, and such ligands would be useful in analyzing binding modes of GH43  $\beta$ -xylosidases. Aminoalcohols could serve this purpose because subsite -1 of SXA is occupied by one glutamic and two aspartic residues that offer potential recognition elements for cations (coulombic interactions). Active-site carboxyl groups have been observed in near proximity to the amino group of tris(hydroxymethyl)aminomethane (Tris) [11,12] and the N group of iminosugars in X-ray structures of other glycoside hydrolases in complex with Tris and iminosugars [13–15]. One of the latter structures has high enough resolution to assign two hydrogen substituents to the imine of an iminosugar to define its cationic state and to assign bond lengths of glutamyl carboxyl groups as deprotonated and anionic for forming favorable electrostatic interactions with the cationic N [15]. For this work, we determined the X-ray structure of SXA in complex with an aminoalcohol and biochemically characterized the binding properties. This constitutes the first structure of a native GH43  $\beta$ -xylosidase in complex with an active-site ligand. Also, we determined the dissociation constant for the SXA homotetramer to its dimers from a sedimentation equilibrium experiment and established that both enzyme forms have similar catalytic properties.

## Materials and methods

### Materials and general methods

4NPX, BTP, inhibitor candidates, and buffers were obtained from Sigma-Aldrich. Water was purified through a Milli-Q unit (Millipore). All other reagents were reagent grade and high purity. A Cary 50 Bio UV-Visible spectrophotometer (Varian), equipped with a thermostatted holder for cuvettes, was used for spectral and kinetic determinations. A model SX.18MV-R stopped-flow (Applied Photophysics), with a thermostatted compartment for syringes and reaction chamber and a 2 mm path length for absorbance measurements, was used for rapid kinetic studies. An AVIV Model 215 circular dichroism spectrophotometer (Aviv Biomedical), equipped with thermostatted cuvette holder, and a 1 mm path length quartz cuvette were used for acquiring protein spectra; three spectra were averaged for each protein sample. Manipulations of coordinates (overlays, distance measurements,

calculations of solvent accessible surfaces, etc.) and molecular graphics images were through the UCSF Chimera package from the Resource of Biocomputing, Visualization, and Informatics at the University of California, San Francisco (supported by NIH P41 RR-01081) [16].

### Protein preparations

Site-directed mutagenesis was performed as described [1,4]. Oligonucleotide primers for the K99A mutant were 5'-GGTCGTAGACGGCATGTGGGCGGATTGTCATAACTACCTG-3' and 5'-CAGGTAGTTATGACAATCCGCCACATGCCGTCTACCACC-3'; the template was pSRA1 with the SXA gene cloned into pET21(+). BL21(DE3) cells producing SXA or SXA K99A mutant were grown and induced as described [1]. BL21(DE3) cells producing selenomethionine-containing SXA were grown similarly with the exceptions that defined media including selenomethionine [18] was used, cells were grown at 25–30 °C and expression of the SXA gene was induced with 1 mM isopropyl- $\beta$ -D-thiogalactopyranoside for 16 h prior to cell harvest. SXA proteins were purified to homogeneity (judged by SDS-PAGE analysis) as described [1], with the addition of a final desalting, gel filtration step employing a 2.6  $\times$  30 cm column of Bio-Gel P-6 DG desalting gel (Bio-Rad), equilibrated and developed with 20 mM sodium phosphate, pH 7.3. K99A SXA and selenomethionine-containing SXA behaved similarly to wild-type SXA in terms of high yields in *Escherichia coli* (~30% of soluble protein) and elution times from chromatography columns. Circular dichroism spectra (190–260 nm, collected for samples containing 8  $\mu$ M enzyme in 20 mM sodium phosphate, pH 7.3) are characterized by a major trough at 214 nm (reflecting dominance of  $\beta$  structure), and the spectra are similar for wild-type SXA and the K99A SXA: mean trough value  $[\theta]$  at 214 nm for two wild-type SXA samples =  $(-2.97 \pm 0.14) \times 10^6$  deg cm<sup>2</sup> dmol<sup>-1</sup>; trough value  $[\theta]$  at 214 nm for the K99A mutant =  $-2.87 \times 10^6$  deg cm<sup>2</sup> dmol<sup>-1</sup>.

### Crystallization and structure determination

Native and selenomethionine-containing crystals of  $\beta$ -D-xylosidase from *S. ruminantium* were obtained from drops containing 4  $\mu$ L of protein solution (1.6 mg/mL in 0.1 M BTP-HCl, pH 8.0) mixed with 1  $\mu$ L of the well solution containing 22–25% (w/v) PEG 1100 monomethyl ether in 0.1 M BTP-HCl, pH 8.0. After about one week of growth, suitable crystals were harvested and flash frozen in liquid nitrogen. Multi-wavelength anomalous dispersive (MAD) data, collected at the selenium peak, edge, and high energy remote, and native data were collected using a MARMOSAIC 225 CCD detector (MarResearch) at the DuPont-Northwestern-Dow (DND) beamline, Sector 5 ID-B of the Advance Photon Source (Argonne, IL). Anomalous diffraction data were processed and scaled using XGEN [19], and native diffraction data were processed and scaled using XDS [20]. Native and selenomethionine-containing crystals are of the same triclinic space group P1 with a homotetramer in the asymmetric unit.

Shake-n-Bake [21] was used to find 28 of 32 possible selenium sites. The initial sites were refined, and initial phases were calculated with MLPHARE [22]. Initial phases, with an overall figure of merit of 0.301, were improved by solvent flattening, phase extension, and 4-fold non-crystallographic symmetry (NCS) averaging, and provided an interpretable electron density map with an overall figure of merit of 0.653 using DM [23]. Automatic model building with ARP/wARP [24] aided with the program Xfit from XtalView [25] correctly built ~95% of the protein. The remaining model was traced manually with COOT [26] alternated with positional refinement against the 1.3 Å native data set using REFMAC5 [27]. Solvent molecules were added with ARP/wARP and alternative positions were added manually and refined with REFMAC5.

### Enzyme-catalyzed reactions

Unless indicated otherwise, reactions were initiated by adding a small aliquot of enzyme (generally 7  $\mu$ L of enzyme diluted into 10 mM sodium phosphate, pH 7.0, and incubated on wet ice or at ~25 °C) to 1-mL temperature-equilibrated (25 °C) reaction mixtures, which were monitored continuously (Cary spectrophotometer) for 0.3 min at 380 nm (for pH values below 6) or 400 nm (for pH values of 6 and above) for determinations of linear initial rates (steady-state rates). Time required for enzyme addition and mixing was 0.2 min prior to collection of rate data. With 4NPA and 4NPX as substrates, initial rates determined from 0.1-s (using stopped-flow instrument) and 30-min reactions were similar [1]. Delta extinction coefficients (product-substrate) used for molar conversion calculations for each reaction condition and end point determinations of 4NPA and 4NPX substrate concentrations were determined as described [1]. Buffers of constant ionic strength ( $I = 0.3$  M), adjusted with NaCl, in the complete reaction mixtures were used as indicated: 100 mM succinate-NaOH (pH 4.3–6), 100 mM sodium phosphate (pH 6–8), 30 mM sodium pyrophosphate (pH 8–10). Discontinuous monitoring of reaction progress for determination of initial rates was conducted as described [1,4]. Values for  $v$  and  $k_{cat}$  are expressed in moles substrate hydrolyzed per second per mole of enzyme active sites (protomers), the latter determined using the calculated extinction coefficient of SXA protomers at 280 nm of 129600 M<sup>-1</sup> cm<sup>-1</sup> [1,28].

Download English Version:

<https://daneshyari.com/en/article/8291987>

Download Persian Version:

<https://daneshyari.com/article/8291987>

[Daneshyari.com](https://daneshyari.com)